


Evidence for octupole correlation in $Z = 50$ Sn isotopes: Spectroscopy of ^{112}Sn

L. Mu (穆琳),^{1,2} S. Y. Wang (王守宇) ,^{1,2,*} G. S. Li (李广顺),³ W. Z. Xu (许文政),^{1,2} Z. P. Li (李志攀),⁴ J. G. Wang (王建国),³ X. C. Han (韩星池),^{1,2} C. Liu (刘晨),^{1,2} A. Rohila,³ H. F. Bai (白洪斐),^{1,2} B. Qi (齐斌),^{1,2} R. N. Mao (毛若楠),⁴ Z. Q. Li (李志泉),^{1,2} X. Xiao (肖骁),^{1,2} L. Zhu (祝霖),^{1,2} X. D. Wang (王旭东),^{1,2} Y. J. Li (李英健),^{1,2} H. Jia (贾慧),^{1,2} R. J. Guo (郭睿巨),^{1,2} Y. D. Fang (方永得),³ Y. H. Qiang (强赞华),³ B. Ding (丁兵),³ M. L. Liu (柳敏良),³ F. F. Zeng (曾凡斐),³ S. Guo (郭松),³ Z. G. Gan (甘再国),³ and X. H. Zhou (周小红)³

¹Shandong Provincial Key Laboratory of Optical Astronomy and Solar-Terrestrial Environment, Institute of Space Sciences, Shandong University, Weihai 264209, People's Republic of China

²WeiHai Research Institute of Industrial Technology of Shandong University, Shandong University, Weihai 264209, People's Republic of China

³Institute of Modern Physics, Chinese Academy of Sciences, Lanzhou 730000, China

⁴School of Physical Science and Technology, Southwest University, Chongqing 400715, China



(Received 18 January 2024; revised 1 February 2024; accepted 24 April 2024; published 10 May 2024)

High-spin states in ^{112}Sn were investigated using the $^{103}\text{Rh}(^{12}\text{C}, 1p2n)$ reaction at a beam energy of 62 MeV. Six electric dipole $E1$ transitions linking positive- and negative-parity intruder bands have been identified in ^{112}Sn through γ -ray spectroscopy. The experimental reduced $E1$ transition probabilities $B(E1)$, derived from level lifetimes by means of the Doppler-shift attenuation method, are of the order of 10^{-4} W.u., which gives evidence for the octupole correlation in ^{112}Sn . The systematics of the reduced $E1$ transition probabilities and neutron energy levels of $5/2^+$ and $11/2^-$ in Xe isotopes suggest an enhanced octupole correlation at neutron number $N = 62$, which is supported by the relativistic Hartree-Bogoliubov calculations.

DOI: [10.1103/PhysRevC.109.L051303](https://doi.org/10.1103/PhysRevC.109.L051303)

Introduction. Semimagic Sn isotopes, where the proton number (Z) is equal to the magic number 50, comprise ten stable isotopes and numerous radioactive isotopes, spanning from $^{100}\text{Sn}_{50}$ to $^{132}\text{Sn}_{82}$. Their basic properties, like masses, binding energies, shapes, and excited states, are indispensable for a detailed understanding and theoretical description of the nuclear system [1–4]. Thereinto, in the study of nuclear shape, Sn isotopes have played an anchor point due to their ground states exhibiting spherical shapes. However, for excited states, the long-range correlations between valence nucleons drive the shape towards deformation. Well-deformed intruder rotational bands built upon $2p$ - $2h$ proton excitations have been observed in even-even $^{106-118}\text{Sn}$ [5–11] and odd- A $^{109-119}\text{Sn}$ [10,12–15] isotopes. These deformed bands were identified as having prolate shapes. In 2001, several $E1$ transitions have been observed between the positive- and negative-parity intruder bands in ^{114}Sn [9]. The obtained $B(E1)$ values in ^{114}Sn were found to be significantly smaller than those in the octupole deformed nuclei $^{142-146}\text{Ba}$, so Ref. [9] suggested that there is no octupole correlation in ^{114}Sn . It is interesting to further explore whether octupole correlations exist in semimagic Sn isotopes.

Octupole correlations in nuclei are generated by the interaction between orbitals of opposite parity near the Fermi surface with orbital (l) and total (j) angular momenta differing by $3\hbar$. More microscopically, these orbitals with $\Delta l = \Delta j = 3\hbar$ could generate octupole interactions only if they

have the same Ω values (assuming no triaxial deformation) [16]. Octupole correlation leads to the reflection asymmetry in the distribution of valence nucleons, thus the centers of charge and mass of an atomic nucleus are separated, and then a sizable electric dipole moment will occur, which will be observable through enhanced $E1$ transitions between opposite parity states [16,17]. Thus, the enhanced $E1$ transitions probabilities (usually taken as $B(E1) > 10^{-5}$ W.u. [16]) is considered as a good indication of octupole correlations. Strong octupole correlations were expected to occur when nucleon numbers are near 34 ($g_{9/2} \leftrightarrow p_{3/2}$ coupling), 56 ($h_{11/2} \leftrightarrow d_{5/2}$ coupling), 88 ($i_{13/2} \leftrightarrow f_{7/2}$ coupling), and 134 ($j_{15/2} \leftrightarrow g_{9/2}$ coupling) [16], which are called “magic” octupole numbers [18]. The single-particle energy spectrum in the octupole-deformed potential exhibits visible energy gaps at these nucleon numbers. These visible shell gaps are attributed to the repulsion of the $\Omega = 1/2$ pair of octupole coupling orbitals [16]. It remains an open question whether higher Ω values of octupole coupling orbitals could open up new energy gaps.

In this Letter, we report on the evidence for octupole correlations in ^{112}Sn and a subshell closure at neutron number $N = 62$ in octupole-deformed potential.

Experimental details. Excited states in ^{112}Sn were populated by the $^{103}\text{Rh}(^{12}\text{C}, 1p2n)$ reaction at a beam energy of 62 MeV at the Heavy Ion Research Facility in Lanzhou (HIRFL). The target consisted of 0.57 mg/cm² isotopically enriched ^{103}Rh backed by a 16.1 mg/cm² lead backing; the backing thickness was sufficient to stop the recoiling nuclei. The emitted γ rays were detected by 17 Compton-suppressed

*sywang@sdu.edu.cn

HPGe detectors and five Compton-suppressed clover detectors. These detectors were placed at five rings with different angles: five clover detectors and two HPGe detectors at 90° , three HPGe detectors at 128° , and four HPGe detectors each at 154° , 52° , and 26° with respect to the beam axis. A total of 3×10^9 γ - γ coincidence events were accumulated. In the off-line analysis, the coincidence events were sorted into several symmetric and asymmetric matrices. The symmetric matrices were used to construct the level scheme and the asymmetric matrices were used to determine the lifetimes of the excited states.

Level lifetimes of bands 1 and 2 in ^{112}Sn were measured using the Doppler-shift attenuation method (DSAM). Lineshapes of γ rays were extracted from the background-subtracted spectra projected from the angle-dependent E_γ - E_γ matrices consisting of events at 154° , 128° , 90° , 52° , and 26° detectors along one axis and all detectors along the second axis. Then, the lifetime analyses were performed using a modified version of the LINESHAPE analysis package [19]. A total of 10^4 Monte Carlo simulations of the velocity history of the recoiling nuclei traversing the target and the backing material were generated in time steps of 0.01 ps. Electronic stopping powers were taken from Ziegler's tabulation [20] with low-energy modifications. A χ^2 minimization for the observed Doppler shifted lineshapes was carried out using the in-band and side-feeding lifetimes, background, and contaminant peak(s) as input parameters. Experimental uncertainties in the extracted lifetimes were determined based on the behavior of the χ^2 fit in the vicinity of the minimum [21–23] by a statistical method using the MINOS [24] program. More details on the fitting procedure can be found in Refs. [21,22,25].

Results and discussions. The partial level scheme of ^{112}Sn derived from the present work is shown in Fig. 1, with two bands labeled as 1 and 2. Thereinto, band 2 consists of two spin branches labeled as a and b. Bands 1 and 2a were previously reported in Refs. [8,26]. In addition to these two bands, a γ -ray cascade of 734, 813, 900, and 974 keV transitions (corresponding to band 2b in this work) belong to ^{112}Sn was also observed in Ref. [26]. It was suggested as the signature partner of band 2a by comparing with the negative-parity coupled band in the neighboring nucleus ^{114}Sn [26]. However, the placement of band 2b was not given in Ref. [26], since its decay path to the other excited states in the level scheme was not found. In the present work, we observed the 1670 keV transition from band 2b to the known 10^- state and the linking transitions between bands 2a and 2b, thus the placement of band 2b is confirmed as shown in Fig. 1. The most intriguing feature of the present level scheme is the observation of six $E1$ transitions between the positive-parity band 1 and the negative-parity band 2. The spectrum in Fig. 2 demonstrates the existences of these $E1$ transitions in ^{112}Sn . More details about the experimental results will be published in a forthcoming paper [27].

Prior to this work, lifetimes of six states in band 1 had already been measured in Ref. [8]. In the present work, in addition to band 1, we also extracted lifetimes of four states in band 2a and three states in band 2b. Representative examples of the fitted lineshapes with the experimental data in the

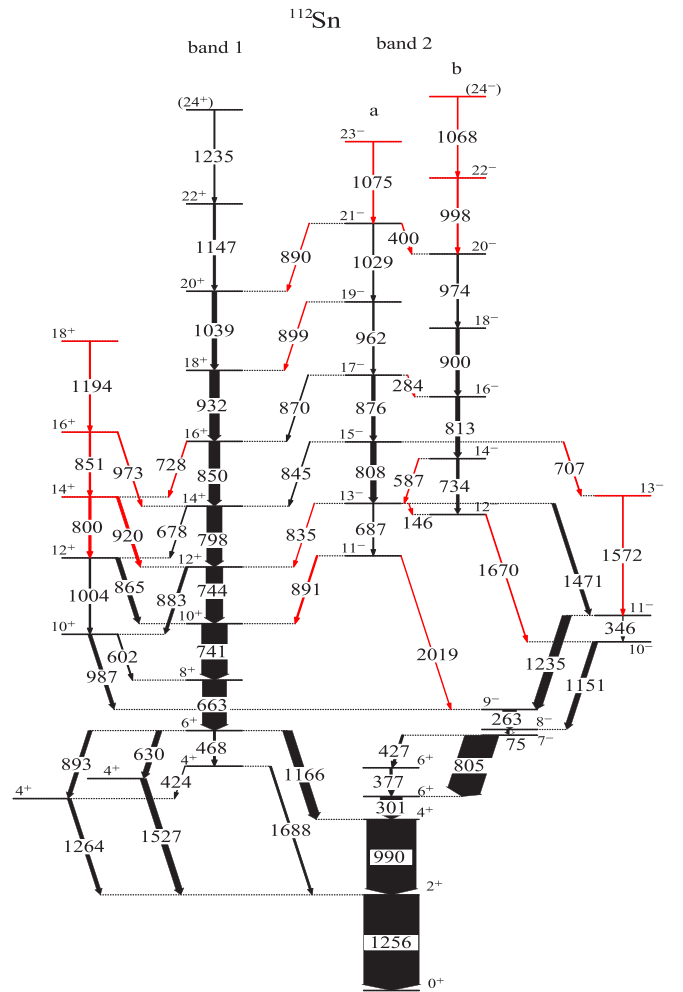


FIG. 1. Partial level scheme of ^{112}Sn derived from the present work. The energies are given in keV, and the widths of the arrows are proportional to the relative transition intensities. New levels and γ -ray transitions are shown in red whereas the known counterparts from the previous works [8,26] are shown in black. Bands 1 and 2 have been respectively assigned as positive- and negative-parity bands in Refs. [8,26], and we adopted these assignments in this Letter. The complete level scheme and the gated spectra showing all new transitions will be published in a forthcoming paper [27].

present work are displayed in Fig. 3. The extracted lifetimes are summarized in Table I, together with the previous results [8]. Systematic errors in the stopping power values are not included in the quoted errors and may be as large as 15% [28]. One can see that the present lifetimes agree within the errors with those from the previous measurements except for the 16^+ level. The reduced transition probabilities $B(E2)$ and $B(E1)$ values were deduced using the expressions [29]

$$B(E2) = \frac{0.0816B_\gamma(E2)}{E_\gamma^5(E2)\tau[1 + \alpha_t(E2)]} (e^2b^2), \quad (1)$$

$$B(E1) = \frac{0.629 \times 10^{-3}B_\gamma(E1)}{E_\gamma^3(E1)\tau[1 + \alpha_t(E1)]} (e^2fm^2), \quad (2)$$

TABLE I. The present measured lifetimes τ , the previous lifetime results in Ref. [8], γ -ray energies (E_γ), the relative intensities (I_γ), and the reduced transition probabilities $B(E2)$ and $B(E1)$ for bands 1 and 2 in ^{112}Sn . Uncertainties in the present measured lifetimes do not include the systematic errors that are associated with the stopping powers, which may be as large as $\pm 15\%$. The relative intensity of the 1256 keV γ ray in Fig. 1 is taken as 100.

band	$I_i(\hbar)$	τ (ps)	τ (ps) [8]	E_γ (keV)	I_γ	$\sigma\lambda$	$B(\sigma\lambda)$ (W.u.)
1	12 ⁺		0.95 ± 0.20	744.3	30.6(3.0)	$E2$	
	14 ⁺	1.53 ^{+0.10} _{-0.03}	1.75 ± 0.40	798.0	27.7(2.7)	$E2$	49 ⁺¹ ₋₄
				677.8	1.5(0.2)	$E2$	6 ⁺² ₋₂
	16 ⁺	1.30 ^{+0.08} _{-0.05}	0.79 ± 0.15	850.4	20.9(2.6)	$E2$	42 ⁺² ₋₃
				728.2	0.9(0.1)	$E2$	4 ⁺¹ ₋₁
	18 ⁺	0.50 ^{+0.02} _{-0.01}	0.49 ^{+0.11} _{-0.14}	932.0	18.2(1.9)	$E2$	72 ⁺² ₋₂
2	20 ⁺	0.35 ^{+0.01} _{-0.01}	0.32 ± 0.08	1038.6	8.8(0.9)	$E2$	60 ⁺² ₋₂
	15 ⁻	0.94 ^{+0.04} _{-0.06}		807.6	10.8(1.1)	$E2$	61 ⁺⁸ ₋₆
				845.1	0.9(0.2)	$E1$	(5 ⁺² ₋₂) × 10 ⁻⁵
				706.7	2.2(0.3)	$E2$	24 ⁺⁸ ₋₅
	17 ⁻	0.73 ^{+0.02} _{-0.02}		875.8	6.8(0.7)	$E2$	58 ⁺⁴ ₋₄
				869.8	0.8(0.1)	$E1$	(9 ⁺² ₋₂) × 10 ⁻⁵
				283.5	0.3(0.1)	$M1/E2$	
	18 ⁻	0.66 ^{+0.06} _{-0.06}		899.9	6.8(0.7)	$E2$	65 ⁺⁷ ₋₅
	19 ⁻	0.56 ^{+0.04} _{-0.04}		961.5	3.5(0.4)	$E2$	49 ⁺⁶ ₋₅
				899.4	0.4(0.1)	$E1$	(11 ⁺⁴ ₋₄) × 10 ⁻⁵
	20 ⁻	0.46 ^{+0.02} _{-0.02}		974.0	2.2(0.2)	$E2$	63 ⁺³ ₋₃
	21 ⁻	0.35 ^{+0.05} _{-0.04}		1029.4	1.3(0.2)	$E2$	39 ⁺¹² ₋₁₀
				890.2	0.3(0.1)	$E1$	(24 ⁺¹⁶ ₋₁₁) × 10 ⁻⁵
				400.4	0.5(0.1)	$M1/E2$	
22 ⁻	0.36 ^{+0.04} _{-0.04}		997.7	1.4(0.2)	$E2$	71 ⁺⁹ ₋₇	

where E_γ , τ , B_γ , and α_t are the γ -ray energy, lifetime, the branching ratio, and the total internal conversion coefficient of the transition, respectively. In the present work, the uncertainties of E_γ and the α_t values (including error) are neglected since they are small compared to the uncertainties of τ and B_γ and have little effect on the $B(E1)$ and $B(E2)$ values.

Band 1, interpreted as the intruder band, has been suggested to have a $2p$ - $2h$ proton excitation across the closed shell at $Z = 50$ with the configuration $\pi(g_{9/2})^{-2}(g_{7/2})^2$ [8]. Around spin 12⁺, the alignment of a pair of $h_{11/2}$ neutrons were identified, and following that, the higher spin states correspond to the $\pi(g_{9/2})^{-2}(g_{7/2})^2 \otimes \nu h_{11/2}h_{11/2}$ configuration [8]. For the

negative-parity bands 2a and 2b, we adopt the interpretation in Ref. [26], that is, they are a pair of signature partner bands similar to the case in ^{114}Sn . Thus, band 2 in ^{112}Sn has the same configuration $\pi(g_{9/2})^{-2}(g_{7/2})^2 \otimes \nu h_{11/2}(g_{7/2}/d_{5/2})$ as that in ^{114}Sn .

Six $E1$ transitions linking bands 1 and 2 have been observed, implying the existence of octupole correlations in ^{112}Sn . In this mass region, octupole correlations are associated with the $h_{11/2}$ and $d_{5/2}$ subshells. As the proton Fermi level lies near the lowest- Ω $g_{7/2}$ orbital far from $h_{11/2}$ orbitals, the occurrence of octupole correlations in ^{112}Sn are more likely arising from the interaction between the neutron $h_{11/2}$ and $d_{5/2}$ orbitals. In general, the observation of enhanced $E1$ strength [usually taken as $B(E1) > 10^{-5}$ W.u.] is often cited as evidence for octupole correlations in nuclei [16]. To study the octupole correlations in ^{112}Sn , the experimental $B(E1)$ values and the energy displacements δE between bands 1 and 2 have been extracted and compared with those in $^{117,121}\text{Xe}$ [30,31] and ^{226}Ra [32] in Fig. 4, which were identified as the typical examples of octupole correlations and stable octupole deformation, respectively. The energy displacement $\delta E = E(I) - [(I+1)E(I-1) + IE(I+1)]/(2I+1)$ is the criteria for determining any degree of octupole deformation. It should be close to zero in the limit of stable octupole deformation. As shown in Fig. 4(a), the $B(E1)$ values are of the order of 10^{-4} W.u. in ^{112}Sn and comparable with those in $^{117,121}\text{Xe}$, but significantly smaller than ^{226}Ra . In Fig. 4(b), the energy displacements δE in ^{112}Sn are also comparable with those in Xe nuclei, but deviate appreciably from those in ^{226}Ra . These results indicate that octupole correlations exist in ^{112}Sn .

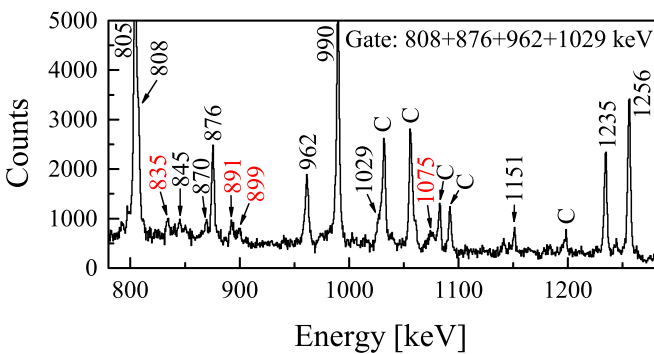


FIG. 2. The γ -ray coincidence spectrum gated on the 808 + 876 + 962 + 1029 keV transitions in band 2a by the detectors at 90°. The newly identified transitions are labeled in red, while the previously known ones are labeled in black. The peaks labeled C indicate contaminations.

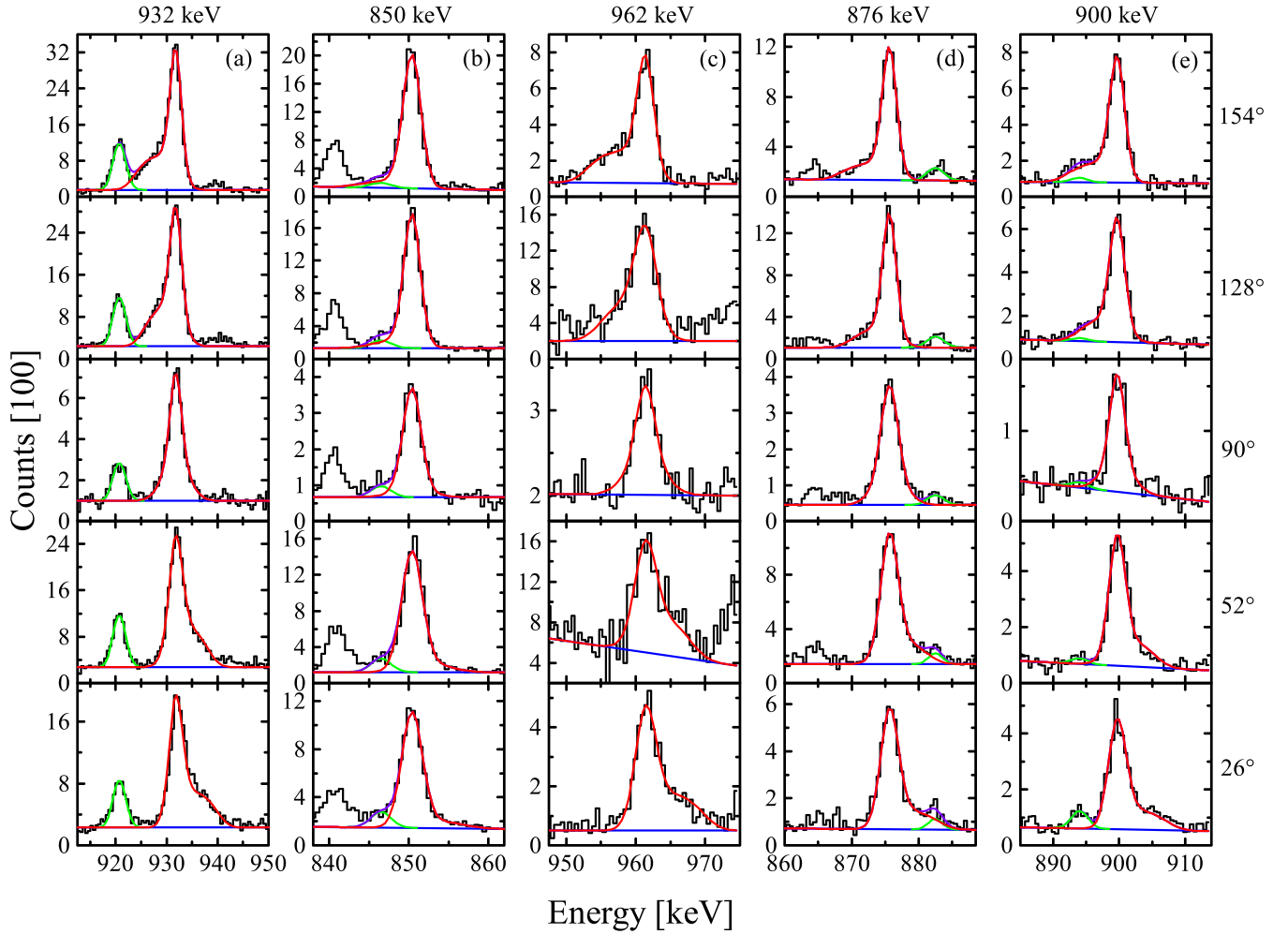


FIG. 3. Representative examples of the lineshape fits for (a) the 932 keV in band 1, (b) the 850 keV in band 1, (c) the 962 keV in band 2a, (d) the 876 keV in band 2a, and (e) the 900 keV in band 2b. Five rows correspond to the angles of 154° , 128° , 90° , 52° , and 26° with respect to the beam direction, respectively. Red line: Doppler broadened lineshape of the analyzed transition. Green line: fitting of the contamination peaks. Violet line: fitting of the all peaks.

In order to investigate the neutron dependence of octupole correlations, we have carried out a systematic study of Xe isotopes as shown in Fig. 5. Thereinto, the information on octupole correlations in the Xe isotopic chain is relatively complete, making it an ideal case to explore the systematics of octupole effects. Figure 5(a) presents the average $B(E1)$ values in even-even Xe [33–36] isotopes. It exhibits the neutron dependence of the $B(E1)$. As shown in Fig. 5(a), $B(E1)$ values of Xe isotopes reach a maximum at $N = 62$ neutrons. Figure 5(b) shows the systematics of $5/2^+$ and $11/2^-$ levels in odd- A Xe isotopes. These levels originate from the neutron $d_{5/2}$ and $h_{11/2}$ orbitals, respectively, which play a major role in octupole correlations. It can be seen that the $11/2^-$ level is closest to the $5/2^+$ level at $N \approx 62$. This feature indicates the $\nu h_{11/2}$ and $\nu d_{5/2}$ orbitals are strongly mixed around $N = 62$, which exactly corresponds to the local enhancement of $B(E1)$ shown in Fig. 5(a). Consequently, the systematics of $B(E1)$ values and neutron levels in Xe isotopes both suggest a local

enhancement of octupole effects around $N = 62$, in addition to the conventional “magic” octupole number 56.

To further study the octupole correlations in ^{112}Sn and the cause of the enhancement in octupole correlation at $N = 62$, we employed the relativistic Hartree-Bogoliubov (RHB) model [37]. Figure 6 shows single neutron levels of ^{112}Sn along a path in the β_2 - β_3 plane, which are obtained from the RHB calculations with the PC-PK1 parametrization [38]. The left panel shows the path which follows the quadrupole deformation parameter β_2 up to 0.25 around the shallow local minimum with the octupole deformation parameter kept constant at zero value. The right panel displays the dependence of the single neutron energies on the octupole deformation from $\beta_3 = 0$ to $\beta_3 = 0.3$, with the constant value $\beta_2 = 0.25$. The necessary condition for the presence of octupole correlation is the existence of pairs of octupole coupling orbitals near the Fermi level. This condition is fulfilled in ^{112}Sn , for which in Fig. 6 one notices states of opposite parity close to the Fermi

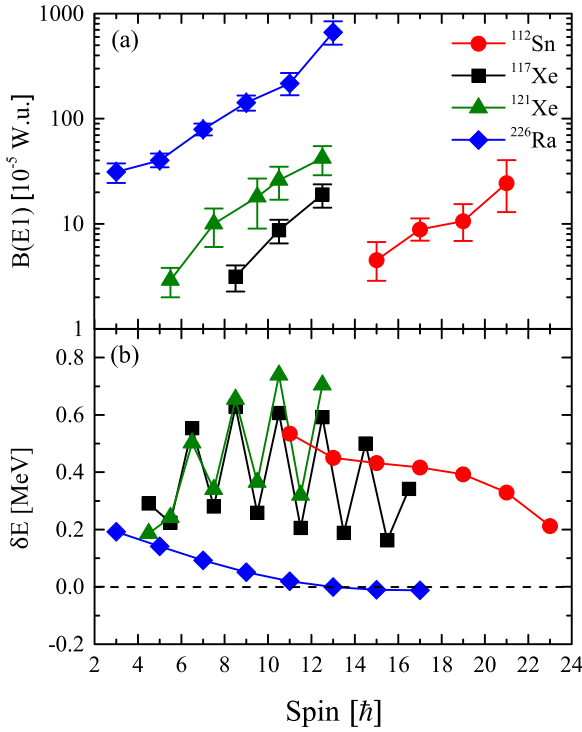


FIG. 4. The experimental $B(E1)$ values (a) and energy displacement δE (b) between the positive and negative parity bands in ^{112}Sn , together with those in $^{117,121}\text{Xe}$ and ^{226}Ra . The data of $^{117,121}\text{Xe}$ and ^{226}Ra are taken from Refs. [30–32].

level, that originate from $d_{5/2}$ and $h_{11/2}$ neutron orbitals. As shown in Fig. 6, the $\Omega = 1/2$ pair of orbitals of the $(d_{5/2}, h_{11/2})$ neutron levels repel each other due to the octupole correlations, thus causing a significant shell gap at “magic” octupole number $N = 56$. In addition, a subshell structure at $N = 62$ which favours the strong octupole correlations also appears in Fig. 6. Unlike the shell closure at $N = 56$, this subshell closure is induced by the repulsion between the $\Omega = 3/2$ pair of orbitals which originate from the $(d_{5/2}, h_{11/2})$ neutron levels. This theoretical calculation supports the enhancement of the octupole correlation at $N = 62$, and explains the cause of the enhancement. This work provides the first evidence for octupole interaction between the $\Omega = 3/2$ orbitals of the $(d_{5/2}, h_{11/2})$ neutron levels.

Summary. In summary, two intruder rotational bands and six $E1$ transitions between opposite parity bands have been identified in ^{112}Sn . The detailed γ -ray spectroscopy with the precise lifetime measurements give the evidence that octupole correlations exist in ^{112}Sn , which was supported by the RHB calculations. The systematics of the $B(E1)$ values and neutron levels suggest that an enhancement of octupole correlation occurs at $N = 62$. The calculated single neutron spectrum reveals that this enhancement is attribute to the octupole correlation between $\Omega = 3/2$ orbitals of $(d_{5/2}, h_{11/2})$ neutron levels. The combination of experimental and theoretical results gives a hint that 62 might be a subshell closure for octupole

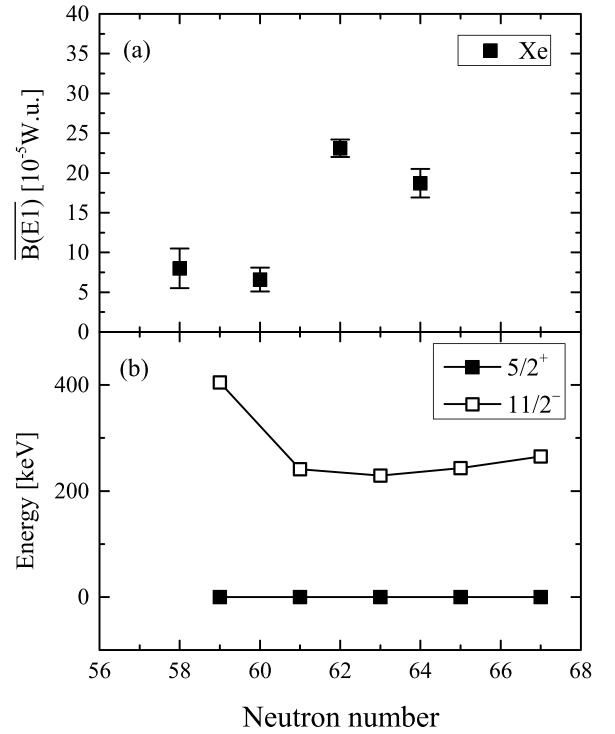


FIG. 5. Systematics of experimental (a) average $B(E1)$ values in even-even Xe isotopes and (b) neutron energy levels of $5/2^+$ and $11/2^-$ in odd-A Xe isotopes originating from $vd_{5/2}$ and $vh_{11/2}$ orbitals, respectively. The $B(E1)$ values of $^{112,114,116,118}\text{Xe}$ are obtained by averaging the available $B(E1)$ values given in the Refs. [33–35]. The data in (b) were obtained from the National Nuclear Data Center (NNDC) database [39].

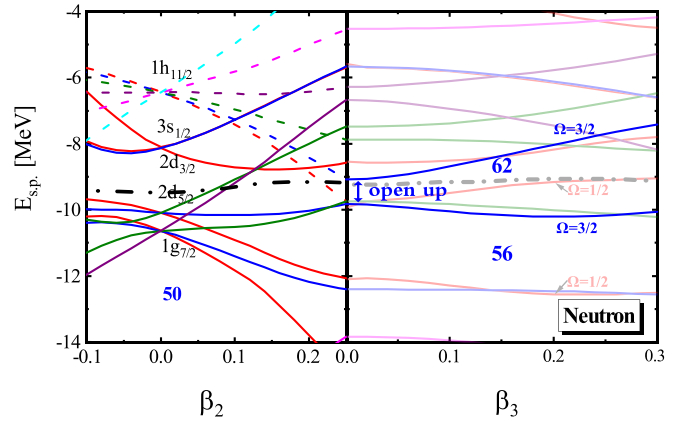


FIG. 6. Single-neutron levels of ^{112}Sn as functions of deformation parameters calculated by the RHB model based on PC-PK1 energy density functional. Each plot follows the quadrupole deformation parameters β_2 up to the position of the equilibrium minimum $\beta_2 = 0.25$ with the constant octupole deformation parameter $\beta_3 = 0$ (left panels). Then, for the constant value $\beta_2 = 0.25$, the panels on the right display the dependence of the single-neutron energies on the octupole deformation, from $\beta_3 = 0$ to $\beta_3 = 0.3$. The thick dash-dotted (black) curves denote the Fermi levels.

correlations and provides the evidence for octupole interaction between the $\Omega = 3/2$ orbitals of the ($d_{5/2}, h_{11/2}$) neutron levels.

Acknowledgments. The authors would like to thank Dr. C.M. Petrache for discussions and valuable comments on the manuscript. This work is partly supported by the National

Natural Science Foundation of China (No. 12225504, No. 12075137, No. 12075138, No. U2167202, and No. 11905113) and the Major Program of Natural Science Foundation of Shandong Province (No. ZR2020ZD30). The authors thank the HIRFL technical staff and accelerator group for their support.

-
- [1] M. Mougeot *et al.*, *Nat. Phys.* **17**, 1099 (2021).
[2] J. Hakala *et al.*, *Phys. Rev. Lett.* **109**, 032501 (2012).
[3] D. Rosiak *et al.*, *Phys. Rev. Lett.* **121**, 252501 (2018).
[4] G. Guastalla *et al.*, *Phys. Rev. Lett.* **110**, 172501 (2013).
[5] R. Wadsworth *et al.*, *Phys. Rev. C* **50**, 483 (1994).
[6] R. Wadsworth *et al.*, *Phys. Rev. Lett.* **80**, 1174 (1998).
[7] H. Harada *et al.*, *Phys. Lett. B* **207**, 17 (1988).
[8] S. Ganguly *et al.*, *Nucl. Phys. A* **789**, 1 (2007).
[9] J. Gableske *et al.*, *Nucl. Phys. A* **691**, 551 (2001).
[10] A. Savelius *et al.*, *Nucl. Phys. A* **637**, 491 (1998).
[11] S. Y. Wang *et al.*, *Phys. Rev. C* **81**, 017301 (2010).
[12] L. Käubler *et al.*, *Z. Phys. A* **356**, 235 (1987).
[13] D. R. LaFosse, D. B. Fossan, J. R. Hughes, Y. Liang, P. Vaska, M. P. Waring, J.-y. Zhang, R. M. Clark, R. Wadsworth, S. A. Forbes, and E. S. Paul, *Phys. Rev. C* **51**, R2876 (1995).
[14] J. M. Sears *et al.*, *Phys. Rev. C* **58**, 1430 (1998).
[15] D. P. Sun *et al.*, *Chin. Phys. C* **46**, 064103 (2022).
[16] P. A. Butler and W. Nazarewicz, *Rev. Mod. Phys.* **68**, 349 (1996).
[17] P. A. Butler, *J. Phys. G: Nucl. Part. Phys.* **43**, 073002 (2016).
[18] I. Ahmad and P. A. Butler, *Annu. Rev. Nucl. Part. Sci.* **43**, 71 (1993).
[19] J. C. Wells and N. R. Johnson, Oak Ridge National Laboratory Report No. ORNL-6689, p. 44, (1991), https://digital.library.unt.edu/ark:/67531/metadc1070831/m2/1/high_res_d/5226283.pdf.
[20] J. Ziegler, *Stopped and Ranges of Ions in Matter* (Pergamon Press, New York, 1980), Vols. 3 and 5.
[21] C. J. Chiara *et al.*, *Phys. Rev. C* **61**, 034318 (2000).
[22] C. J. Chiara *et al.*, *Phys. Rev. C* **64**, 054314 (2001).
[23] N. Johnson *et al.*, *Phys. Rev. C* **55**, 652 (1997).
[24] F. James and M. Roos, *Comput. Phys. Commun.* **10**, 343 (1975).
[25] A. D. Ayangeakaa *et al.*, *Phys. Rev. Lett.* **110**, 102501 (2013).
[26] M. Schimmer *et al.*, *Nucl. Phys. A* **539**, 527 (1992).
[27] L. Mu *et al.* (unpublished).
[28] S. Mukhopadhyay *et al.*, *Phys. Rev. C* **78**, 034311 (2008).
[29] H. Ejiri and M. J. A. de Voigt, *Gamma-Ray and Electron Spectroscopy in Nuclear Physics* (Clarendon Press, Oxford, 1989), Chap. 6.
[30] E. S. Paul *et al.*, *Nucl. Phys. A* **644**, 3 (1998).
[31] J. Timár *et al.*, *J. Phys. G: Nucl. Part. Phys.* **21**, 783 (1995).
[32] H. J. Wollersheim *et al.*, *Nucl. Phys. A* **556**, 261 (1993).
[33] J. F. Smith *et al.*, *Phys. Lett. B* **523**, 13 (2001).
[34] G. de Angelis *et al.*, *Phys. Lett. B* **535**, 93 (2002).
[35] J. M. Sears, D. B. Fossan, G. R. Gluckman, J. F. Smith, I. Thorslund, E. S. Paul, I. M. Hibbert, and R. Wadsworth, *Phys. Rev. C* **57**, 2991 (1998).
[36] S. Törmänen *et al.*, *Nucl. Phys. A* **572**, 417 (1994).
[37] W. Sun, S. Quan, Z. P. Li, J. Zhao, T. Niksic, and D. Vretenar, *Phys. Rev. C* **100**, 044319 (2019).
[38] P. W. Zhao, Z. P. Li, J. M. Yao, and J. Meng, *Phys. Rev. C* **82**, 054319 (2010).
[39] NNDC, National Nuclear Data Center, Brookhaven National Laboratory, <http://www.nndc.bnl.gov>.